Pol. J. Environ. Stud. Vol. 31, No. 6 (2022), 5765-5779
DOI: *10.15244/pjoes/152381* ONLINE PUBLICATION DATE: 2022-10-18

Original Research

Polyphenols Content, Chelating Properties and Adsorption Isotherms and Kinetics of Red and Yellow Pomegranate Peels (*Punica granatum* L.) Towards Lead (II)

Lina Abed, Noureddine Belattar*

Laboratory of Applied Biochemistry, Faculty of Nature and Life Sciences, Ferhat Abbes University, Setif 1, 19000 Setif, Algeria

Received: 2 May 2022
Accepted: 25 July 2022

Abstract

Metal pollutants produced by industrial wastewaters have become a global concern given their impact on the environment and human health. The purpose of this study was to assess the polyphenols content and the iron chelating activity in the peels of two pomegranate varieties. After the biomass characterization via FT-IR, point of zero charge and surface functional groups analysis, the lead adsorption was then investigated by batch method. Finally, the regeneration of the biomasses was performed by acidic desorption. Polyphenols content of the red peels extract was higher than the yellow one; 102.9±0.9 and 85.9±1.3 mg GAE/g of dry weight, respectively with a half iron chelation inhibitory concentration (IC_{50}) of 227.2±1.7 and 235.9±3.2 µg.mL^{-1} of extract, successively. For the adsorption isotherms of lead onto the red and yellow pomegranate peels, the Langmuir model was more fitting with an adsorption capacity (Q_{max}) of 90 and 89.25 mg.g^{-1}, respectively. The kinetic data corresponded better to the pseudo-second order model. The acidic desorption of lead was successful with a high percentage of recovery. The results demonstrate the effectiveness of these biomasses as biosorbents for lead removal from aqueous solutions with the possibility of their reuse.

Keywords: pomegranate peel, polyphenols content, adsorption isotherms, adsorption kinetic, lead removal

Introduction

Environmental pollution is a world-wide concern that can cause the deterioration of the spheres of earth. Consequently, it is urgent today more than ever, to mitigate the degradation of the abiotic sphere (air, water and soil) or the biotic sphere (plants, animals and microorganisms), which interact in cycles and any damage caused to the first one impacts the last one. In fact, intensive agriculture, industrialization and globalization have altered the balance of the ecological system by introducing organics and metals compounds

*e-mail: nbelattar@yahoo.com

which are very deleterious to nature and the lives of humans and animals. The environment has been tainted by numerous pollutants such as inorganic ions, organic pollutants, radioactive elements, gaseous pollutants and nanoparticles [1-2].

Heavy metals such as arsenic, cadmium, chromium, lead and mercury are considered among the main metals with a severe impact on the balance of the environment with their dangerous consequences on human health given their high degree of toxicity and deleterious effects [3]. The exposure of humans to these metals has been substantially increased by industrial activities linked to the needs of various technologies. Lead is present in the crust of earth and in all compartments of the abiotic sphere, it is one of the most used metals in batteries accumulators manufacturing and metal extraction and finishing activities [4]. In developing countries and in view of the lack of occupational safety measures, many workers continue to be exposed to the toxic effects of lead. Lead contamination is more likely to affect children younger than 6 years old, which can gravely affect their mental and physical development [5]. In terms of absorption, humans are exposed to lead by different ways, in particular orally route via ingestion of contaminated food, drinks and water resources or indirectly through polluted soil. Inhalation is a second major pathway of exposure to airborne lead in the form of micro particles. This route is more dangerous than the first one because the micro particles penetrate deep into the respiratory tract and increase the exposure rate [6].

After absorption, several sensitive organs are affected by the toxicity of lead accumulation such as hematological, immune, cardiovascular, nervous and reproductive systems. Kidneys, liver and bone marrow can also be affected [6-7]. The lead toxicities are responsible for several diseases such as increased blood pressure, kidney diseases, neurodegenerative diseases and cognitive disorders. Furthermore, given the systemic toxicity, the lead has been classified as a possible human carcinogen [8]. It's well known that oxidative stress is an imbalance between antioxidants and oxidants that produces harmful reactive oxygen species (ROS), which is the main mechanism involved in heavy metal toxicity and carcinogenicity [9]. In effect, lead is able to deregulate the antioxidant defenses barriers, including the antioxidant enzymes and the non-enzymatic antioxidants and thus affect the cellular integrity and the metabolism of the cells constituents [10]. In addition, metal ions have been shown to interact with DNA and nuclear proteins, causing their damage through mutation or deletion that can lead to cell cycle modulation and carcinogenesis [11].

In view of the extremely serious effects of metal pollution on the environment and its impact on the ecological balance and on human health in particular, it is therefore urgent to clean up the industrial sources of these polluted effluents before discharging them into the environment. For that, different technologies of treatment have been used and evaluated based on various chemical or physical methods such as precipitation, adsorption on minerals, filtration using membranes and electrochemical methods. A comparison between these technologies is shown in Table 1 [12-16]. Adsorption constituted an effective alternative way to these methods in removing metal pollutants due to its elevated efficiency, reduced operating costs and simplicity of use [17]. Every year, agricultural and agro-food activities release very large quantities of by-products which truly constitute a source of plant biomasses to solve the problem of heavy metal pollution due to their abundance, cost-effective and high efficiency in removing pollutants without side effects on the environment. In fact, a large number of reported studies have been conducted to valorize biomasses as sorbents for heavy metal species from aqueous solutions such as olive stones from olive meal waste waters and apricot shells waste from fruit juice industry, which are potential sorbents for several metal ions [18-19]. Moreover, various plant peels have been used efficiently in the adsorption of different metals such as lead on potato and banana peels [20-21]. Finally, a previous study established that *Nigella sativa* L. seeds biomass preliminarily defatted as a potential sorbent for lead from aqueous solutions and wastewaters from battery factories [22].

Pomegranate (*Punica granatum* L.) is a fruit that has been cultivated for a long time worldwide. Its consumption as it is or as a juice has increased given its health benefits. Consequently, its production and processing were increased simultaneously, which generated massive quantities of peels as a major by-product. Pomegranate peels, in addition of their cellulosic matrix, have a high content of bioactive compounds belonging to polyphenolic secondary metabolites such as phenolic acids, flavonoids and hydrolysable tannins that possess numerous biological activities in particular antioxidant and chelating properties. In this context, the objective of this work was primarily to establish the polyphenols content of two varieties of pomegranate peels and their iron chelating activity. The adsorptive properties of these biomasses as biosorbent towards Pb(II) ions, which is the predominant metal ion in battery factory and lead refining effluents, were also assessed in the second step.

The adsorption study was conducted by batch method using synthetic aqueous solutions by varying the concentration of this metal, contact time, pH and sorbent doses. The adsorption isotherms models and kinetics of Pb(II) ions at interface were also established. Fourier Transform Infrared Spectroscopy (FT-IR) analysis was used to characterize the identity of the functional groups of these biomasses in both native and adsorbed states. Finally, the adsorption-desorption capacity was also carried out by batch method, using a given amount of these biomasses for lead removal from simulated solution that mimics the content

Table 1. Comparison of different techniques used for metal removal from wastewaters.

Technique	Material	Advantages	Disadvantages
Chemical precipitation	Precipitants like sulfide, calcium oxide, Sodium hydroxide and carbonate.	Simplicity of use, applicable for low metal concentration and large volumes of effluents.	It requires pH maintenance at optimum levels, high dosage of chemicals, monitoring of different factors (pH, metal concentration, temperature etc.) during the process.
Coagulation and flocculation	Coagulants like aluminum, ferrous sulfate and ferric chloride. Focculants such as polyaluminum chloride, polyferric sulfate and polyacrylamide.	Sludge settling. Suitable for high volumes of wastewaters.	High cost of reagents, toxicity of inorganic coagulants and the production of large volume of sludge which creates disposal issues.
Electro-chemical methods	Electrodes based on carbon, sulfur, iridium oxide-coated titanium and aluminum etc.	High efficiency, lower chemical use and the recovery of pure metal.	High capital and running costs. Not suitable for large volumes of wastewaters.
Ion exchange	Natural materials like inorganic zeolites or synthetic materials such as ionic resins supported by membranes.	Selectivity of metal removal and the possibility of the regeneration of materials.	High operational costs and partial removal of metals.
Membrane filtration	Membranes with different porosities and surfactants to help the process.	Selective separation and possibility of wastewaters recovery which prevent environmental issues.	Membranes clogging and high capital and operational costs.
Reverse osmosis	Semi-permeable membranes like Thin film composite aromatic polyamide and cellulose acetate.	Simple and effective for metal removal from wastewaters.	Requires constant maintenance due to the risk of degradation and fouling of membranes.
Adsorption	Carbon-based adsorbents like activated carbon nanoparticles [13]. Chitosan-based adsorbents [14]. Mineral adsorbents like zeolites [15].	Lower operating costs, high removal efficiency, easy and simple application. Regeneration of the biosorbent and recovery of metal.	No regeneration. Costs of activated carbon.
Biosorption	Like ripe black locust seed pods [16]. Pomegranate peels (current study).		Early saturation of the biosorbents. Costs for chemical regeneration of the adsorbent.

in real effluents of the battery factory and then acidic regeneration was attempted in order to investigate its reusability for further cycles.

Material and Methods

Chemicals and Equipment

All the chemicals and solvents used in the various experiments in this study were analytical grade. Lead nitrate $Pb(NO_3)_2$ purchased from Prolabo (France), deionized water (20 $\mu s.cm^{-1}$) obtained from ENPEC (National Company of Electrochemical Products, Algeria) were used in achieving adsorption experiments. Sodium chloride (NaCl, 99.4%, Sigma), sodium hydroxide (NaOH, 98%, Cheminova) and hydrochloric acid (HCl, 37%, Biochem) were used in chemical characterization. For total polyphenols quantification and the iron chelating activity; Folin-Ciocalteu reagent, sodium bicarbonate (Na_2CO_3), gallic acid, ferrozine (2,4,6-Tris-2-pyridyl-s-triazine) and methanol (99.8%) obtained from Sigma-Aldrich were used.

The pH measurement was determined by a glass electrode (Hanna HI 9321). Atomic absorption spectrophotometer (AAS) (PerkinElmer PinAAcle 900H model) working with an air acetylene flame was used to estimate the content of lead in the tested solutions. FT-IR spectrophotometer (SHIMADZU FTIR – 8400S), was used to identify the functional groups of the biomasses in native and binding sorbate-sorbent states.

Biomass Adsorbents

Two pomegranate peels, red and yellow, used in this study were prepared from *Punica granatum* fruit purchased from the local market of Setif (East part of Algeria). In the laboratory, the fruits were washed with tap water and then with distilled water to ensure the removal of dirt or unwanted matter. The peels were obtained by extraction of the juice from the arils and discarding their seeds and then dried in the oven at 40ºC for 72 hours until a constant weight was obtained. The dried peels were first grounded to a fine powder and then sieved to obtain a particle size of 500 µm. The raw peels powder was kept in sealed bottles away from the dark at room temperature until their use in adsorption experiments.

Preparation of Stock Solution

Stock solution (1000 mg.L^{-1}) of lead was prepared by dissolving lead nitrate $Pb(NO_3)_2$ in deionized water. The working solutions were prepared by diluting the stock solution to appropriate volumes. The initial pH value of the solutions was adjusted using 0.1 M sodium hydroxide NaOH or 0.1 M hydrochloric acid HCl.

Polyphenols Quantification

At first, we proceeded to extract the polyphenolic compounds from the peels powder at room temperature by maceration in aqueous solution with a ratio of 1/10 (W/V) during 24 hours under agitation. The filtrate was collected by filtration under vacuum using fritted glass (G3) and then, the remaining solid phase was subjected to a second extraction under the same conditions for 12 hours to ensure complete recovery of polyphenols. The two filtrates were combined and dried at 40°C until a dry residue was obtained that was kept away from the light and moisture. The determination of total polyphenols is carried out according to Le et al. [23], which is based on the reduction in an alkaline medium of Folin-Ciocalteu reagent by the oxidizable groups of the phenolic compounds. Briefly, 200 µL of the extract was mixed with 1 mL of Folin-Ciolcalteu reagent (10%). After 4 min, 800 µL of sodium carbonate solution (75 g.L^{-1}) was added followed by incubating the mixture in the dark and at room temperature for 2 h and then, the absorbance was measured at 765 nm with UV-Vis spectrophotometer. A calibration curve was constituted using gallic acid as a reference. The concentration of polyphenols was determined and the results were expressed in mg equivalents of gallic acid per g of dry weight (mg GAE/g DW).

Iron Chelating Activity

The iron chelating activity was estimated through the ability of the extracts to inhibit the iron(II)–ferrozine complex formation based on the method described by Le et al. and Ibrahim et al. with some modifications [23-24]. Concentrations ranging between (0.0075-1.2 mg.mL^{-1}) of the aqueous extracts for both RPP and YPP were tested, in which 0.5 mL of the extract was mixed with 0.05 mL of $FeSO_4$ (2 mM in distilled water). After 5 minutes, 0.05 mL of ferrozine (5 mM in 80% methanol) was added. The mixture was then shaken and incubated for 10 minutes at room temperature and the absorbance of the complex was measured at 562 nm against a reagent blank. The Na_2EDTA (0.001-0.005 mg.mL^{-1}) was used as a standard metal chelating agent. The control was prepared with the same manner by replacing the extract with distilled water. The chelating activity percentage was calculated using the following equation:

$$\text{Chelating activity (\%)} = \frac{A_C - A_E}{A_C} \times 100$$

Where, A_C is the absorbance of the control and A_E is the absorbance of the extract or Na_2EDTA. The results were expressed as mg of EDTA equivalent/g of extract.

Characterization of the Adsorbent

The Equilibrium pH of the Adsorbent

The contact pH of the adsorbent was established by mixing 0.25 g of the pomegranate peel powder in contact with 25 mL of deionized water. The whole was kept under agitation for 24 h. After 24 h the suspension was filterd and the pH of the filtrate was determined using a pH meter [25-26].

Point of Zero Charge (pH_{pzc})

The point of zero charge was determined using the salt addition method. In a series of 50 mL conical flasks 25 mL of sodium chloride NaCl 0.01 M was added in each flask. The initial pH (pH_i) was adjusted between 2 to 12 using either NaOH 0.1 M or HCl 0.1 M. After adjusting the pH, 25 mg of the peel's powder (500 µm) was added to every flask. The samples were left under agitation for 24 h at room temperature. After 24 hours, the final pH of each sample was measured and marked as pH_f. The PZC was obtained from the plot of $\Delta pH = (pH_f - pH_i)$ against pH [27].

Surface Functional Groups

The concentration of acidic and basic sites on the pomegranate peel was determined via the acid-base titration method [28]. Thus, 0.25 g of the adsorbent was treated separately with 25 mL of 0.5 M NaOH and 0.5 M HCl in 50 mL conical flasks for the determination of acid and basic surface functional groups, respectively. The flasks were agitated at room temperature for 24 h. Subsequently, the suspensions were decanted and filtered. 10 mL of each filtrate was taken and the excess acid or base was back-titrated with 0.5 M NaOH or HCl. The number of functional groups was calculated taking into account that the NaOH neutralizes the phenolic, lactonic and carboxylic groups and HCl neutralizes the basic groups. The total acidity and basicity was expressed in mmol.g^{-1} of adsorbent [29].

FT-IR Analysis

The FT-IR spectrums of the red peels powder (RPP) and the yellow peels powder (YPP) before and after Pb(II) ions adsorption were taken to establish

wavenumber changes in the functional groups of the adsorbents. The FT-IR spectra were recorded between 400 and 4000 cm^{-1}.

Adsorption Studies

Batch Biosorption Studies

The biosorption capacity of RPP and YPP towards lead ions (Pb^{2+}) was studied using batch method at room temperature (23-25ºC). The working solutions were prepared by diluting the stock solution (1000 $mg.L^{-1}$) with deionized water to appropriate concentrations and their initial pH was adjusted using 0.1 M sodium hydroxide NaOH or 0.1 M hydrochloric acid HCl. For this study, a fixed amount of the peels powder (0.0025-0.02 g) was placed in a 15 mL flasks containing 10 mL of the metallic lead solution in the range of 5 to 100 $mg.L^{-1}$ at a given pH from 2 to 8 for a contact time varying from 15 to 120 min and then, the flasks were shaken in a rotary orbital shaker at 70 rpm. Finally, the flasks were centrifuged at 3000 rpm for 10 min followed by filtration through 0.45 µm filters. The experiments were carried out in triplicate. The residual concentration of metal ions in the filtrate was determined using atomic absorption spectrophotometer. The amount of metal ions sorbed by the biosorbent and the percentage of removal (R%) were calculated using the following equations:

$$Q_e = \frac{(C_e - C_0)\times V}{m} \quad (1)$$

$$R\% = \frac{(C_0 - C_e)\times 100}{C_0} \quad (2)$$

Where, Q_e is the amount of heavy metal ions adsorbed per unit weight of the biomass ($mg.g^{-1}$); V is the volume of solution (L); C_0 is the initial lead metal ion concentration ($mg.L^{-1}$); C_e is the equilibrium lead concentration ($mg.L^{-1}$) and m is the mass of the biosorbent (g).

Adsorption Isotherms Models

The adsorption isotherm is a mathematical description of the relationship between the amounts of the solute adsorbed on the adsorbent and the concentration of dissolved adsorbate in the liquid at equilibrium and at a constant temperature. The adsorption equilibrium takes place when the concentration of adsorbate in the solution is in dynamic balance with that of the interface. The parameter C_{eq} corresponds to the concentration of the metal ion remained in the solution and Q_{eq} refers to the amount of metal ion adsorbed per unit weight of adsorbent [22, 30]. Our experimental data were adjusted to the models of Freundlich and Langmuir, which are the most frequently used models in the literature. The adsorption of Pb(II) ions at optimum pH (6) and agitation time (60 min) was accomplished at different Pb(II) ions concentrations ranging from 10 to 4000 $mg.L^{-1}$ and a biosorbent dose of 0.02 g at ambient temperature.

Langmuir Isotherm

Langmuir models propose that adsorption occurs on adsorbent surfaces with a monomolecular layer structure in which all adsorption sites are identical and there is no contact between the molecules that have been adsorbed [31]. The Langmuir equation is given as follows:

$$Q_e = \frac{Q_m K_L C_e}{1 + K_L C_e}$$

The linear form of Langmuir isotherm equation is:

$$\frac{C_e}{Q_e} = \frac{C_e}{Q_m} + \frac{1}{Q_m K_L}$$

Where Q_e is the equilibrium concentration of Pb(II) ions on the biosorbent ($mg.g^{-1}$), Q_m is the theoretical maximum adsorption capacity ($mg.g^{-1}$), C_e is the equilibrium concentration of Pb(II) ions ($mg.L^{-1}$), and K_L is the Langmuir constant ($L.mg^{-1}$). The values of Q_m and K_L constants and coefficients of regression for Langmuir isotherm are obtained from the plot of C_e/Q_e versus C_e illustrated by Fig. 7.

The important characteristic of the Langmuir isotherm is the dimensionless constant separation factor or the equilibrium parameter, R_L, given as follows:

$$R_L = \frac{1}{1 + bC_0}$$

The value of R_L gives an idea about the form of the isotherm. When it is $R_L>1$ it indicates an unfavourable isotherm, $R_L = 1$ indicates a linear isotherm, $0<R_L<1$ indicates a favourable isotherm, while $R_L= 0$ indicates an irreversible adsorption [32].

Freundlich Isotherm

Freundlich models propose that the molecules are adsorbed as a monomolecular layer or multilayer structure on heterogeneous adsorbent surfaces and that there is contact between the molecules that have been adsorbed [33]. The Freundlich equation is given as follows:

$$Q_e = K_f C_e^{1/nf}$$

The linear form of Freundlich isotherm equation is:

$$\text{Log } Q_e = \text{Log } K_f + \frac{1}{n_f} \text{ Log } C_e$$

Where K_f is the Freundlich isotherm constant ($mg.g^{-1}$ $(L.mg^{-1})^{1/n}$), nf is the adsorption intensity, C_e is the equilibrium concentration of Pb(II) ions ($mg.L^{-1}$) and Q_e is the equilibrium concentration of Pb(II) ions on the biosorbent ($mg.g^{-1}$). K_f and n_f are Freundlich constants and they represent the adsorption capacity and the adsorption intensity, respectively. The values of K_f and n_f are obtained from the slope and intercept of the plot Log Q_e against Log C_e [32].

Kinetics Modeling

The study of the adsorption kinetics is essential to design the appropriate adsorption process and it gives valuable data on the adsorption rate, the adsorbent behavior and the mass transfer technique [34]. Two kinetic models such as the Lagergren-first order and pseudo-second-order were used in this study to describe the adsorption kinetics. Adsorption capacity Q_t was determined using the following equation:

$$Q_t = (C_0 - C_t) \times \frac{V}{m}$$

Where Q_t is the amount of heavy metal ion adsorption per unit weight of the biomass at time t ($mg.g^{-1}$),C_0 and C_t are Pb(II) ions concentrations ($mg.L^{-1}$) at initial time and time t, respectively, V is the volume of the solution (L) and m is the mass of biosorbent (g).

The Pseudo-Frst-Order Kinetic

The pseudo-first order model equation is for the adsorption in a liquid-solid system. It considers that one ion is adsorbed on top of one adsorption site [35-36].

The Lagergren equation is given as follows:

$$\frac{dQ_t}{dt} = K_1 (Q_e - Q_t)$$

The linear form of pseudo-first order model equation is:

$$\text{Log } (Q_e - Q_t) = \text{Log } Q_e - K_1 t$$

Q_e and Q_t represent the concentration of Pb(II) ions on the biosorbent at equilibrium and at time t, respectively ($mg.g^{-1}$), K_1 is the first-order model constant (min^{-1}). K_1 and Q_e are obtained from the slope and intercept of the plot Log $(Q_e - Q_t)$ versus t (Fig. 8).

The Pseudo-Second-Order Kinetic

The pseudo-second-order model equation is founded on chemisorption and proposes that one ion is adsorbed on top of two adsorption sites [36-37]. The equation is given as follows:

$$\frac{dQ_t}{dt} = K_2 (Q_e - Q_t)^2$$

The linear form of pseudo-second order model equation is:

$$\frac{t}{Q_t} = \frac{1}{K_2 Q_e^2} + \frac{1}{Q_e} \times t$$

Where Q_e and Q_t are the concentration of Pb(II) ions on the biosorbent at equilibrium and at time t, respectively ($mg.g^{-1}$), K_2 is the second-order model constant ($g.mg^{-1}.min^{-1}$). K_2 and Q_e are obtained from the slope and intercept of the plot t/Q_t versus t (Fig. 8).

Batch Desorption Studies

Desorption studies constitute a very interesting step in the process of depollution of wastewaters that allow to elucidate the nature of the interactions between sorbate and sorbent at interface and by the same way to evaluate the possibility to regenerate the adsorbent for its reuse, which has a positive impact in economic terms. Desorption experiments were performed by using a simulated solution of Pb(II) at a concentration that mimics its real content in the wastewaters of ENPEC factory (National Company of Electrochemical Products, Setif, Algeria) preliminarily determined by atomic spectrophotometry. For that, 10 mL of Pb(II) solution at 50 $mg.L^{-1}$; which represents approximately twice the amount in the effluents of this factory (22 $mg.L^{-1}$), were mixed with 0.02 g of biosorbent for 1 hour under stirring at ambient temperature. This procedure was repeated for 3 cycles in order to determine the actual adsorption capacity of the biomass under optimum conditions.

After each cycle, the collected supernatant was centrifuged at 3000 rpm for 10 min and filtrated on 0.45 µm filters, then the residual Pb(II) content was determined as previously mentioned for quantifying the amount of total lead adsorbed. Before carrying out the desorption after the third cycle, the lead-loaded biosorbent was first washed with deionized water to remove the free non-adsorbed fraction, then 10 mL of the desorbing or the eluting solution of 1 M hydrochloric acid (HCl) was added and the mixture was stirred during 15, 30, 60 and 120 min. Finally, the amount of desorbed Pb(II) ions in the supernatant was measured as before to allow an evaluation of the desorption rate.

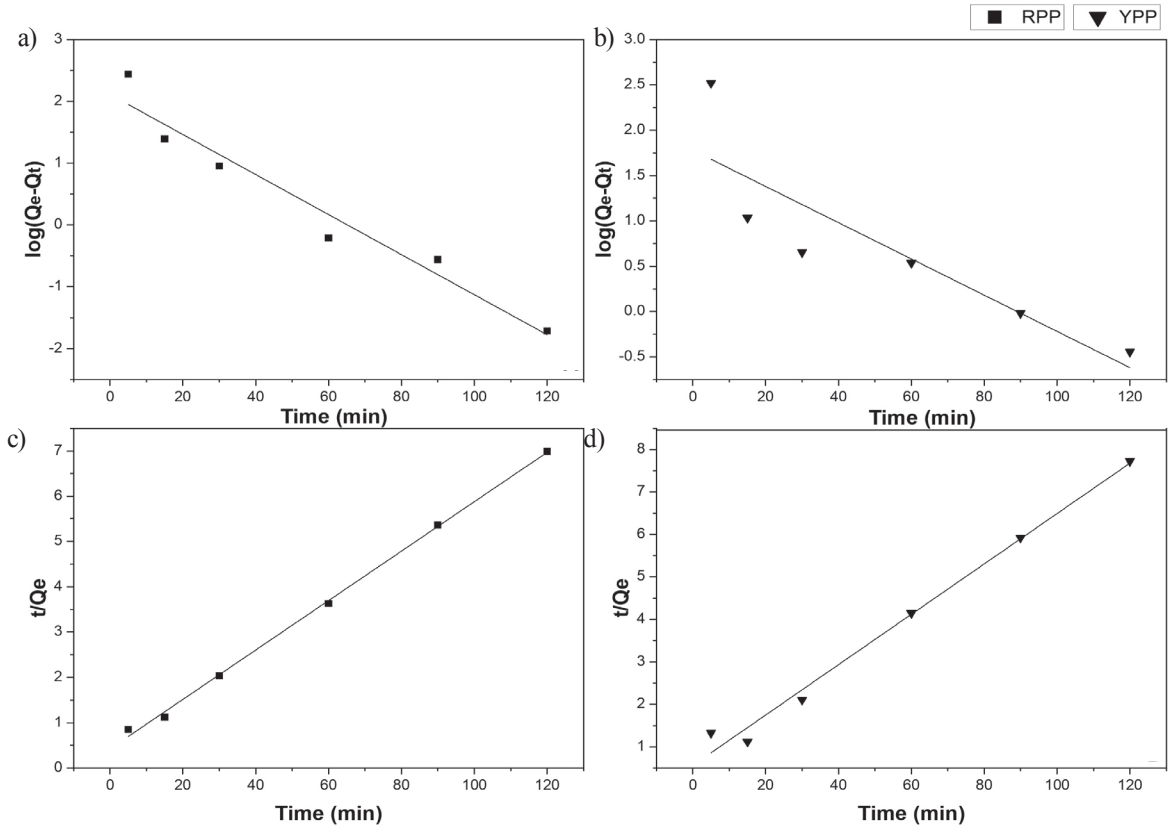

Fig. 7. Linear plots of isotherms for Pb(II) ions adsorption onto pomegranate peel: a) RPP Freundlich isotherm b) YPP Freundlich isotherm c) RPP Langmuir isotherm d) YPP Langmuir isotherm (Pb(II) dosage = (10 to 4000 mg.L^{-1}), RPP and YPP dosage = 20 mg at pH 6.0 and for 60 min).

Statistical Analysis

The results were given as the mean±SE for three replicates for each sample. The IC_{50} value for the iron chelating activity assay was calculated by linear regression analysis.

Results and Discussion

Polyphenolic Content and Iron Chelating Activity

The results of total polyphenols content are presented in Table 2. The RPP extract had greater concentration of TPC 199.1±0.9 mg GAE/g (102.9±0.9 mg GAE/g DW) than the YPP extract which had 184.2±1.3 mg GAE/g of extract (85.9±1.3 GAE/g DW). Other studies reported comparable TPC results of pomegranate peel aqueous extracts [38-39], which were 242.05±7.99 and 178.25±6.22 mg GAE/g of the extract, respectively.

The chelating activity is estimated by the power of extracts to inhibit the formation of Fe^{2+}-ferrozine complex. At a concentration of 1.2 mg.mL^{-1}, The RPP extract showed a ferrous ion chelating capacity slightly higher than the YPP extract with 77.4±0.5% and 76.5±0.7%, respectively. In regard to IC_{50} values, RPP extract had better chelating activity 227.2±1.7 µg.mL^{-1} compared to YPP extract 235.9±3.2 µg.mL^{-1}, which could be explained by the difference in polyphenols content between the two extracts (Table 2). These results were greater than the ones found by Orak et al. in the peel's aqueous extracts of four pomegranate varieties ranging from 40% and 68.55% at a concentration of 1 mg.mL^{-1} [40]. The methanolic peel extracts of different pomegranate cultivars tested by Fawole et al. revealed similar chelating capacity with 67.02% to 83.56% at the same concentration [41]. At a concentration of 0.05 mg.mL^{-1}, Na_2EDTA (used as a standard) showed a great ferrous ion-chelating capacity 96.9±0.3% with an IC_{50} of 7.1±0.03 µg.mL^{-1}.

Characterization of the Adsorbent

The Equilibrium pH of the Adsorbent

The contact pH of the RPP and YPP were found to be 4.20 and 4.08, respectively. These pH values inform about the adsorbents acidic nature and confirm the Boehm titration results.

Point of Zero Charge (pH_{pzc})

The pH_{pzc} of the RPP and YPP was 5.11 and 4.55 respectively (Fig. 1). Therefore, below the pH_{pzc}

Table 2. Total phenolic content (TPC) and iron chelating activity of the RPP and YPP extracts. Results are (means±SE) (n = 3). GAE (gallic acid equivalent).

Sample	TPC (mg GAE/g DW)	Fe^{2+}chelating activity IC_{50} ($\mu g.mL^{-1}$)	Fe^{2+}chelating activity (mg EDTA equiv/g extract)
RPP extract	102.9±0.9	227.2±1.7	31.25
YPP extract	85.9±1.3	235.9±3.2	30.09
EDTA	-	7.1±0.03	-

the surface of the biosorbent is protonated by an excess of protons (H^+) thus, positively charged. Above pH_{pzc}, the surface of the biosorbent is negatively charged due to its deprotonation by the presence of (OH^-) ions in the solution. Tunisian pomegranate peel adsorbent had similar pH_{pzc} value of (4.7) [25]. However, Indian pomegranate peel adsorbent had higher pH_{pzc} value of (7) [42], these variations can be explained by the differences in the ratio between acidic and basic functional groups in each variety.

Surface Functional Groups

The total concentration of the acidic functional groups (carboxylic, phenolic and lactonic) on the surface of the RPP and YPP adsorbents was 18.5 $mmol.g^{-1}$ and 16 $mmol.g^{-1}$, which is more important than the concentration of the basic functional groups with 4 $mmol.g^{-1}$ and 2 $mmol.g^{-1}$ for the RPP and YPP, respectively.

FT-IR Analysis

The FT-IR analysis of RPP and YPP before and after Pb(II) ions adsorption is shown in Fig. 2(a-b). For the net powder RPP and YPP, the peaks at 3405 cm^{-1} can be assigned to the stretching vibrations of hydroxyl group (OH) which confirms the presence of carboxylic acids, polysaccharides of cellulose, phenolic compounds and evidently traces of water. The peaks at 1735 cm^{-1} indicates the carbonyl group (C=O) stretching vibration which can be attributed to the CO bonds in cellulose. The peaks at 1620 and 1623 cm^{-1} can be assigned to the bending of amino group (N–H).The peaks at 1339 and 1352 cm^{-1} can be attributed to the in-plane bending of hydroxylic group (OH). The bands around (1231-1232 cm^{-1}) and (1032-1036 cm^{-1}) can be due to the stretching vibrations of carbonyl group (C–O). These results matches well with the ones found earlier by Boehm titration, thus pomegranate peel powder is rich in acidic functional surface groups that can interact with Pb(II) ions. Earlier studies showed similar spectra of pomegranate peel powder [43-44]. However, the spectra of the peel powder after adsorption pbRPP and pbYPP showed that the intensities of the peaks were increased as well as the shifting of some bands. This indicates the possible involvement of carbonyl, hydroxyl, carboxyl and amino groups that characterize the biosorbents in the adsorption process.

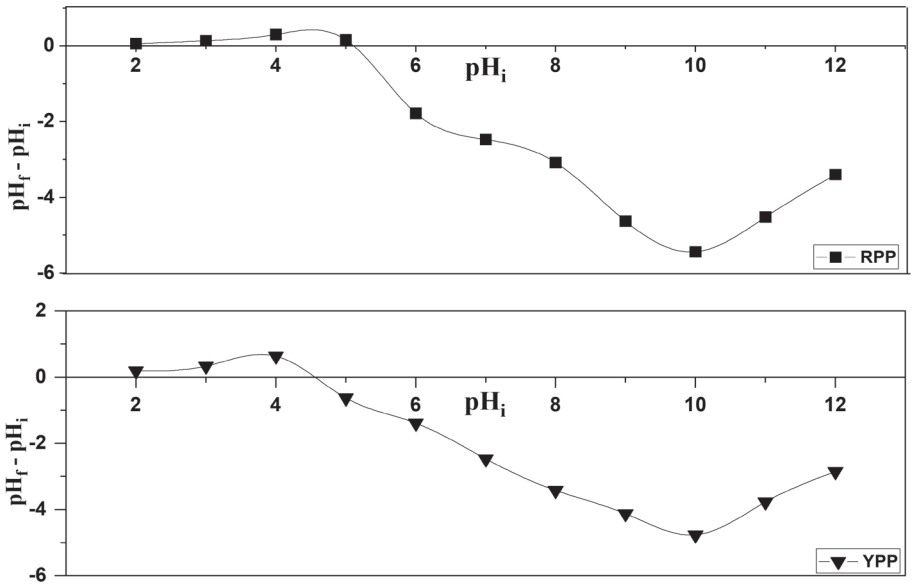

Fig. 1. Point of zero charge (pHpzc) of RPP and YPP.

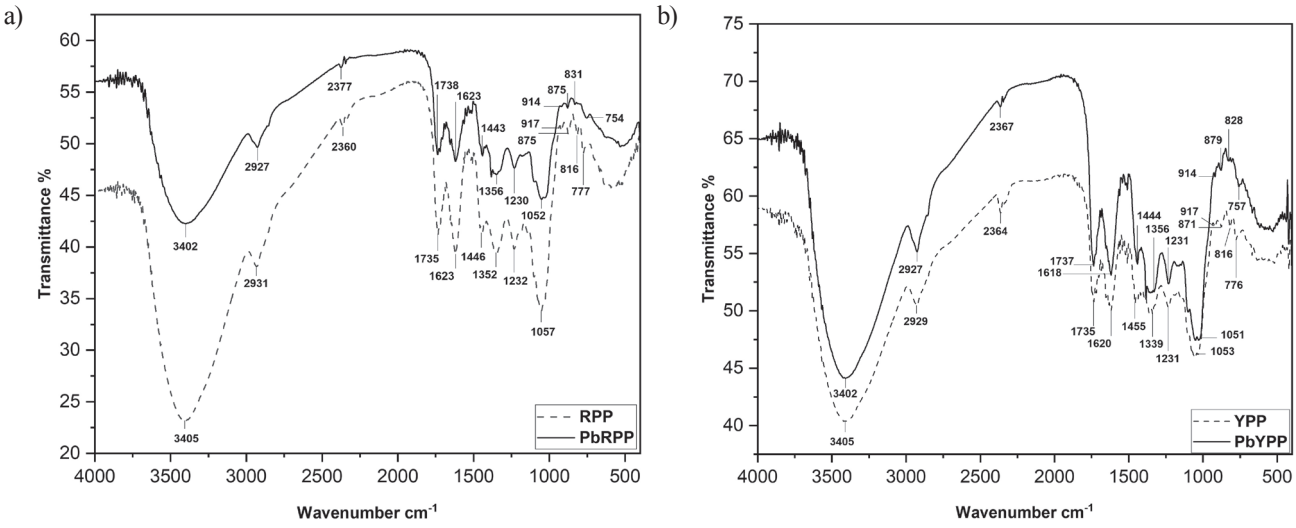

Fig. 2. a) Infrared spectra of RPP, b) Infrared spectra of YPP.

Adsorption Studies

pH Effect

The pH is a crucial element that has an impact on the adsorbent metal uptake and the biosorption mechanism because it affects the ionization of the surface functional groups and the speciation of metal ions. The effect of pH on the Pb(II) ions adsorption was studied by varying the pH from 2 to 8 (Fig. 3). There was an increase in the adsorption capacity of the biosorbent with the increase in pH from 2 to 5 and it attained a maximum adsorption capacity (Q_e) at pH 6 with 18.89 and 17.53 mg.g^{-1} for the RPP and YPP, respectively. Then, it decreased after pH 6 until it reached 15.5 and 15.1 mg.g^{-1} at pH 8 for the RPP and YPP, consecutively.

At acidic pH values, more protons are present in the medium; therefore they compete with the Pb(II) cations for the adsorption sites, so the biosorbent surface would be strongly linked with protons H^+. As the pH increases, the concentration of protons decreases and the surface functional groups of the biosorbent become negatively charged, this makes the biosorbent surface more attractive for metal cations adsorption, thus increasing the adsorption capacity of the biosorbent.

The pH can also affect the metal ion speciation, Pb(II) from pH 2 up to 6 remains with the positive charge, but over pH 6, the Pb^{2+} species concentration decreases remarkably and the concentrations of other lead species increases $Pb(OH)^+$, $Pb_3(OH)_4^{2-}$ and $Pb(OH)_2$ and the hydroxide ions (OH^-) which causes the precipitation of Pb(II) in the form of $Pb(OH)_2$ [45]. In the same manner, the working pH could affect the biosorbent charge. In effect, this pH (6) is above the point of zero charge of the biosorbent (pH_{pzc}) 5.11 and 4.55 for the RPP and YPP, respectively. Thus, the surface of the biosorbent is negatively charged which favorize the adsorption of lead cations. The results obtained in this study are in a good agreement with those reported in previous studies using pomegranate peel powder for heavy metals removal [25, 42, 46].

Time Effect

In view of the obtained results, the adsorption of Pb(II) ions increased rapidly between the time of (0-15 min) and then increased slowly to attain equilibrium within 60 min (Fig. 4). Any further increase in contact time had no significant effect on the concentration of Pb(II) adsorbed for both RPP and YPP. Thereby, the contact time for subsequent batch experiments was chosen to be 60 min.

Biosorbent Dose Effect

The biosorption of the Pb(II) was studied in batch mode, varying the mass of the biosorbent from 2.5 to

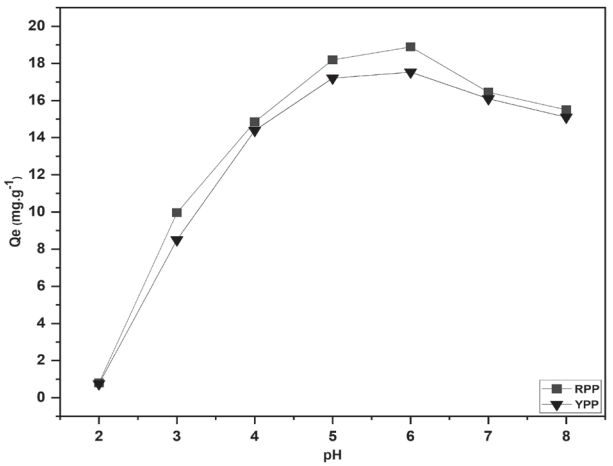

Fig. 3. pH effect on the adsorption of Pb(II) ions onto pomegranate peel (Pb(II) dosage = 25 mg.L^{-1}, RPP and YPP dosage = 10 mg at pH from 2.0 to 8.0 and for 60 min).

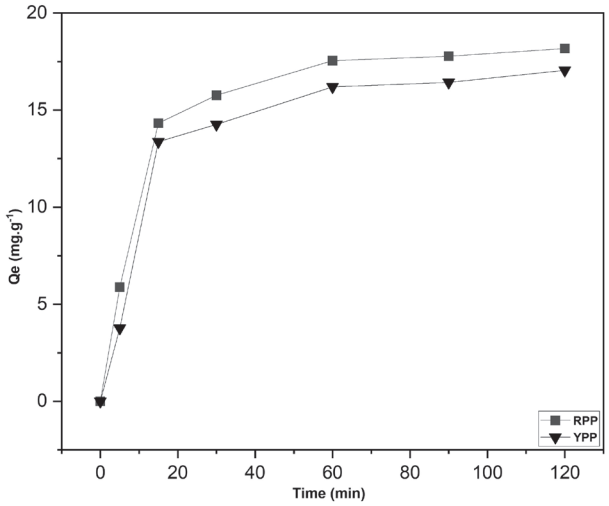

Fig. 4. Time effect on the adsorption of Pb(II) ions onto pomegranate peel (Pb(II) dosage = 25 mg.L^{-1}, RPP and YPP dosage = 10 mg at pH 5.5 and for 0 to 60 min).

20 mg. The adsorption experiments were done with 10 mL of Pb(II) ions at a concentration of 25 mg.L^{-1}, at a pH of 5.5 and at room temperature. The obtained results shows that the Pb(II) ions removal efficiency increases as the biosorbent dose increases. In fact, the rate of Pb(II) ions removal at a dose of 2.5 mg was 59.2% and 58.5% for RPP and YPP, respectively. At high dose of 20 mg, this rate reached 76.4% and 74.6% for both biosorbents, successively (Fig. 5). This can be explained by the disponibility of more adsorption sites. In contrast, the Pb(II) ions biosorption capacity (Q_e) went from 9.55 and 9.33 mg.g^{-1} at a dose of 20 mg to 59.16 and 58.48 mg.g^{-1} at a dose of 2.5 mg for RPP and YPP, respectively (Fig. 5). Thus, the biosorption capacity is inversely proportional to biosorbent dose. Therefore, its increase leads to a direct decrease in adsorption capacity due to the unsaturation of the adsorption sites [47-48].

Initial Metal Concentration Effect

The influence of the initial metal concentration on the adsorption capacity of the YPP and YPP was studied for concentration values of 5, 10, 20, 40, 60, 80 and 100 mg.L^{-1} at pH 5.5 for 60 min at ambient temperature. Fig. 6 shows that the adsorption capacity increased with increasing initial Pb(II) ions concentration; the adsorption capacity increases from 2.81 mg.g^{-1} and 2.49 mg.g^{-1} to 50.8 mg.g^{-1} and 49.1 mg.g^{-1} when the initial metal concentration increases from 5 mg.L^{-1} to 100 mg.L^{-1} for the RPP and YPP, respectively. At low concentrations, Pb(II) ions are adsorbed to a limited number of sites, while with the increase of Pb(II) ions concentration, more sites are occupied, showing that the initial metal concentration plays an important role in the adsorption capacity of Pb(II) ions on the biosorbent [43].

Adsorption Isotherms

The adsorption parameters (Table 3), estimated from the isotherm plots (Fig. 7), show that both Langmuir and Freundlich models fit well with the experimental data. However, the theoretical adsorption capacity of

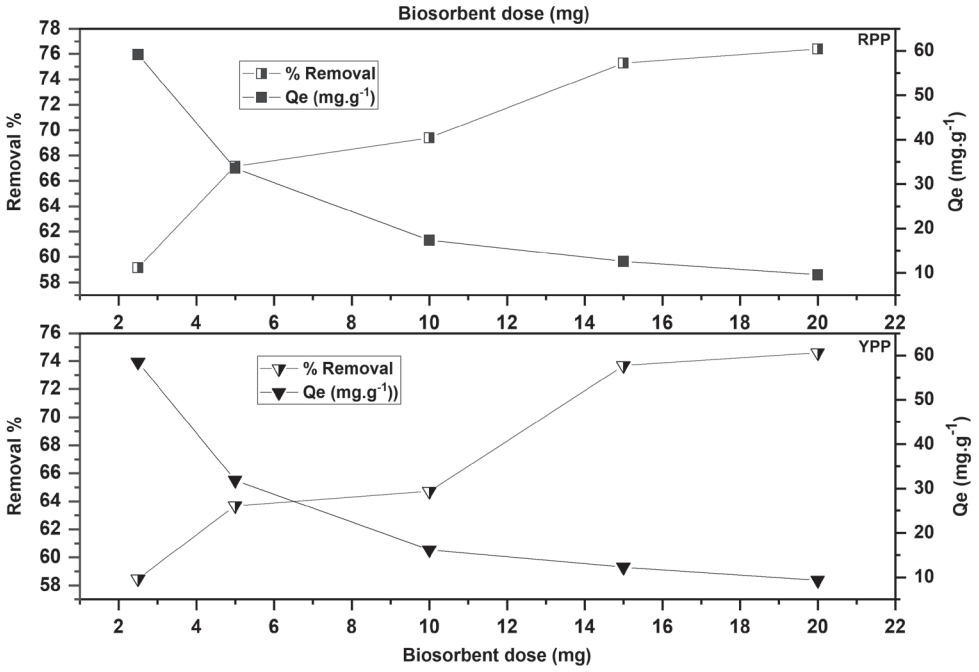

Fig. 5. Biosorbent dose effect on lead removal efficiency and on the adsorption of Pb(II) ions onto pomegranate peel (Pb(II) dosage = 25 mg.L^{-1}, RPP and YPP dosage = from 2.5 to 20 mg at pH 5.5 and for 60 min).

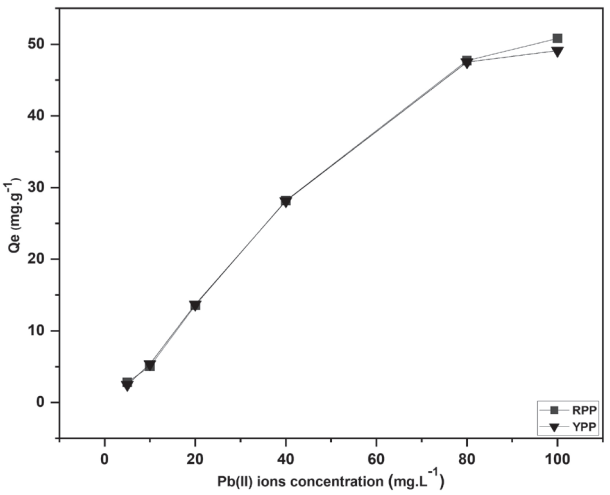

Fig. 6. Initial metal concentration effect on the adsorption of Pb(II) ions onto pomegranate peel (Pb(II) dosage = 5 to 100 mg.L^{-1}, RPP and YPP dosage = 10 mg at pH 5.5 and for 60 min).

the Pb^{2+} ions (Q_{max}) 91.32 mg.g^{-1} and 91.07 mg.g^{-1} for RPP and YPP, respectively found in Langmuir model are in conformity with the experimentally determined adsorption capacity (Q_e) 90 mg.g^{-1} and 89.25 mg.g^{-1} for RPP and YPP , successively. Effectively, the coefficient of correlation (r^2) in Langmuir model is closer to 1 than the one found in Freundlich model. These results are lower than the ones found by Ay et al. on the behavior study of pomegranate peels towards lead ions with Q_{max} = 166.63 mg.g^{-1} [39], but the work conducted by Ben-ali et al. on the adsorption of copper ions by pomegranate peels showed higher results with Q_{max} = 20.49 mg.g^{-1} [25]. Moreover, the separation factor R_L is in the range of [0.016-0.872] for the RPP and [0.018-0.884] for YPP which is under <1, suggesting a favorable adsorption of the Pb(II) ions onto the RPP and YPP adsorbents. As shown in Table 3, in Freundlich model 1/n<1 for both RPP and YPP which means that the Pb(II) ions adsorption is favorable on both biosorbents. Finally, these parameters suggest that the Langmuir isotherm is the better fit for describing the adsorption mechanism than the Freundlich model. The study established by Pavan et al. on the uptake of lead ions by ponkan peels revealed better results than the pomegranate peels with a maximum adsorption capacity of Q_{max} = 112.1 mg.g^{-1} [49]. Similar results were detected by Isaac and Sivakumar using custard apple fruit shell as biosorbent for lead ions with a maximum uptake of Q_{max} = 90.93 mg.g^{-1} [50]. However, the banana peels analyzed by Anwar et al. showed a low maximum adsorption capacity towards lead ions Q_{max} = 5.71 mg.g^{-1} [51].

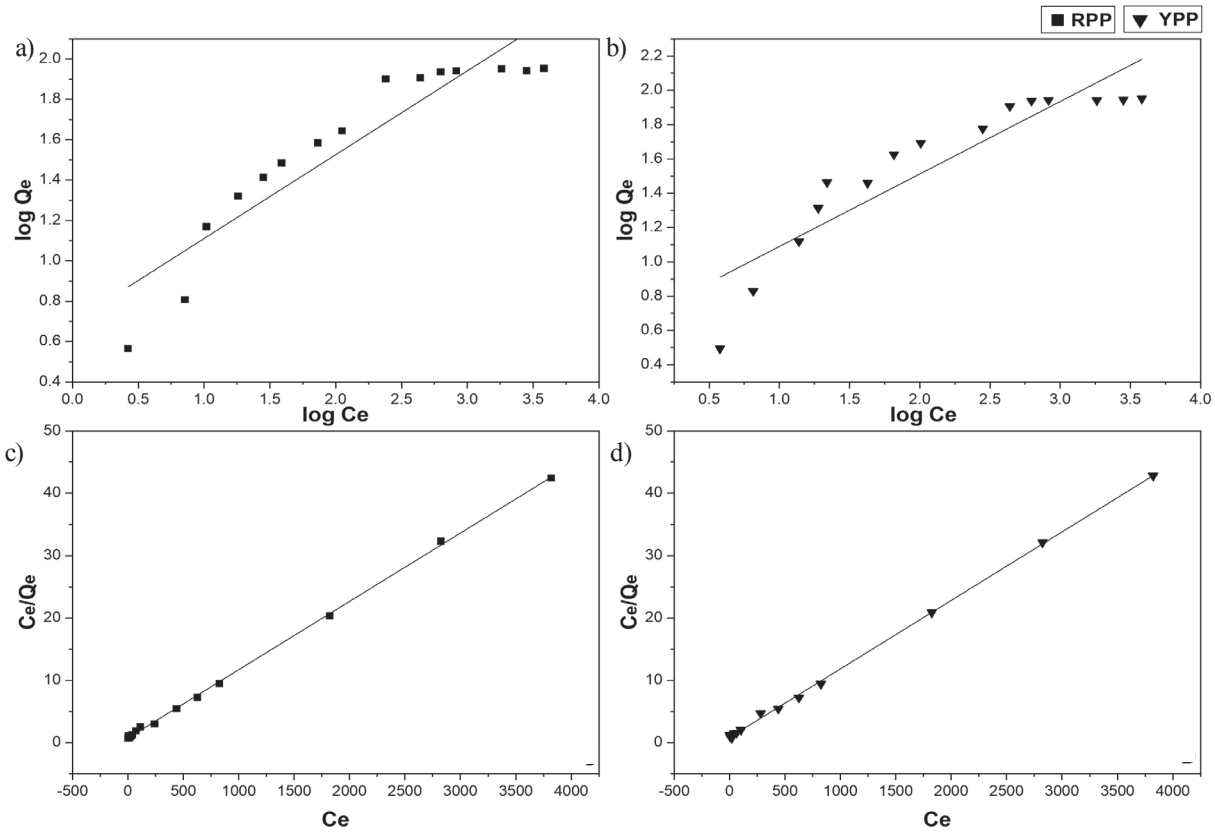

Fig. 7. Linear plots of isotherms for Pb(II) ions adsorption onto pomegranate peel: A) RPP Freundlich isotherm B) YPP Freundlich isotherm C) RPP Langmuir isotherm D) YPP Langmuir isotherm (Pb(II) dosage = (10 to 4000 mg.L^{-1}), RPP and YPP dosage = 20 mg at pH 6.0 and for 60 min)

Table 3. Isotherm parameters of Pb(II) ions onto pomegranate peel RPP and YPP.

Material	Langmuir					Freundlich		
	$Q_{max\ (experimental)}$ ($mg.g^{-1}$)	$Q_{e\ (calculated)}$ ($mg.g^{-1}$)	K_L ($L.mg^{-1}$).	R_L	r^2	K_F ($mg.g^{-1}$ $(L.mg^{-1})^{1/n}$)	1/n	r^2
RPP	90.00	91.3242	0.0146	[0.016-0.872]	0.99933	2.0034	0.4153	0.8516
YPP	89.25	91.0746	0.0130	[0.018-0.884]	0.99931	1.9473	0.4226	0.8210

Table 4. Kinetic parameters of Pb(II) ions onto pomegranate peel RPP and YPP.

Material	Pseudo first-order kinetic model				Pseudo second-order kinetic model			
	$Q_{e\ (experimental)}$ ($mg.g^{-1}$)	$Q_{e\ (calculated)}$ ($mg.g^{-1}$)	K_1 (min^{-1})	r^2	$Q_{e\ (experimental)}$ ($mg.g^{-1}$)	$Q_{e\ (calculated)}$ ($mg.g^{-1}$)	K_2 ($g.mg^{-1}.min^{-1}$)	r^2
RPP	17.35	8.25	0.03239	0.94026	17.35	18.35	0.00700	0.99818
YPP	16.18	5.92	0.01998	0.71271	16.18	16.88	0.00623	0.98662

Adsorption Kinetics

Given the calculated parameters of kinetics models shown in Table 4, it appears that the pseudo-second order fits the experimental data better than the pseudo-first order (Fig. 8), in view of the similarity between the experimental (Q_e = 17.35 and 16.18 $mg.g^{-1}$) and the calculated (Q_e = 18.35 and 16.88 $mg.g^{-1}$) Pb(II) ions

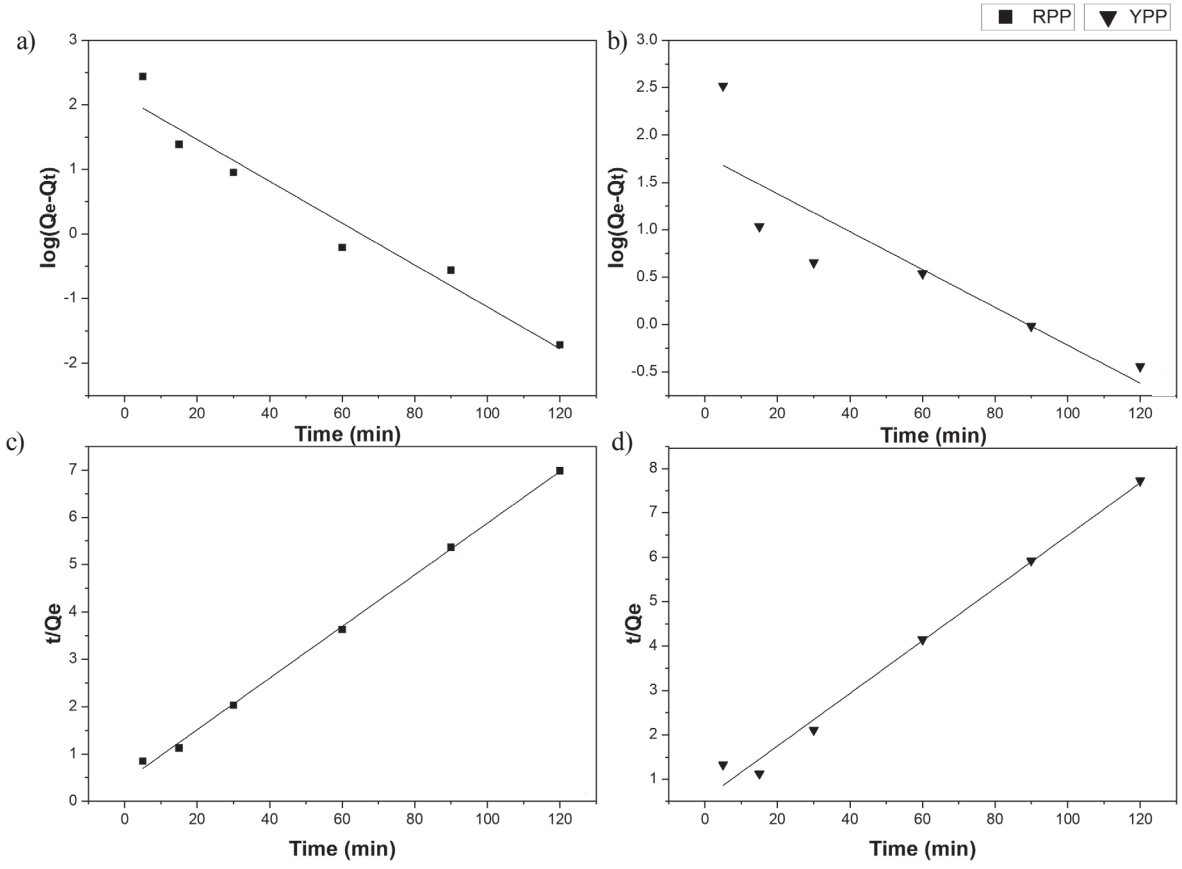

Fig. 8. Kinetic linear plots for Pb(II) ions adsorption onto pomegranate peel: A) RPP pseudo-first order model B) YPP pseudo-first order model C) RPP pseudo-second order model D) YPP pseudo-second order model (Pb(II) dosage = 25 $mg.L^{-1}$), RPP and YPP dosage = 10 mg at pH 5.5 and for (0 to 120 min)).

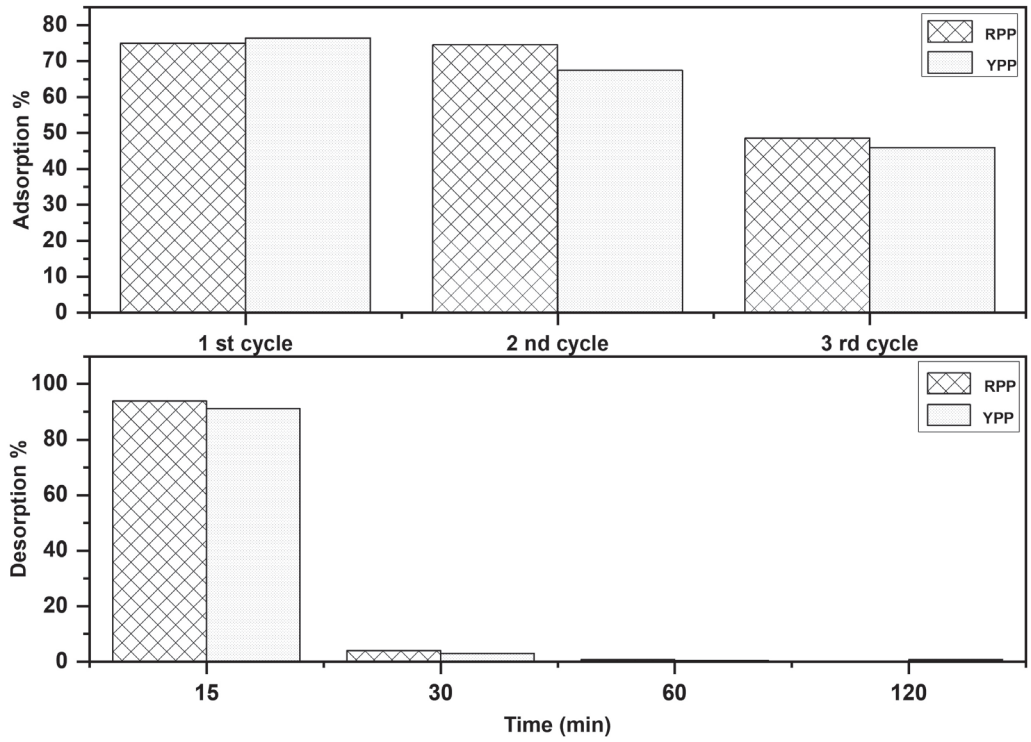

Fig. 9. Desorption of Pb(II)-loaded pomegranate peel biosorbents using 1 M HCl for 15 to 120 min (after 3 cycles of adsorption with Pb(II) solution of 50 mg.L^{-1} per cycle, RPP and YPP dosage = 20 mg at pH 6.0 for 60 min).

adsorption capacity (Q_e) for RPP and YPP, respectively. In addition, the pseudo-second order model has the highest regression coefficient r^2; (0.99818) for the RPP and (0.98662) for the YPP. Therefore, the adsorption of Pb(II) ions onto the studied biosorbents follows the pseudo-second order model. Former studies assessed on the adsorption of lead ions onto pomegranate peel waste exhibited matching results [43, 52].

Desorption Studies

The aim of the simulated industrial wastewater lead removal tests is to determine what volume of real wastewater can be treated by the two biosorbents and their regeneration for Pb(II) ions adsorption. Adsorption capacity of the RPP and YPP was similar for the first and the second cycle; 74.98%, 74.54% and 76.4%, 67.44%, respectively. After the third cycle, the adsorption capacity decreased by 26.44% and 30.46% for the RPP and YPP, successively contrasted to the first cycle (Fig. 9). As to the desorption process, the majority of Pb(II) ions was desorbed after 15 to 30 min with a cumulative percentage of 97.89% for the RPP and 94.13% for the YPP as shown in Fig. 9. The rest of the chelated lead was desorbed within the next 60 and 120 minutes. These results show that both yellow and red pomegranate peels are effective and efficient adsorbents for Pb(II) ions removal from real industrial effluents with a potential of their regeneration which allows their reusability.

Conclusions

The results of this work are part of the global flow to counter the serious effects of environmental pollution by lead and its impact on human health. At first we determined that the yellow and red peels of the pomegranate have an appreciable content of polyphenols in the order of 85.9±1.3 and 102.9±0.9 mg GAE/g of dry weight with a dose dependent iron chelating activity of 30.09 and 31.25 mg EDTA Eq/g extract, respectively.

In terms of adsorption, these two biomasses have high capacities towards lead metal ions, at optimum conditions and at equilibrium, compared to various biosorbents of microbiological or plants nature with Q_e of 89.25 mg.g^{-1} and 90 mg.g^{-1} for the yellow and red ones respectively. These experimental values are well correlated with the theoretical ones, calculated according to the Langmuir model, in which the maximum adsorption capacities of lead (Q_{max}) are 91.32 mg.g^{-1} and 91.07 mg.g^{-1} with a correlation coefficient close to 1. This adsorption at interface is elsewhere favorable given the value of the obtained separation factor (R_L<1). The kinetics studies showed that the experimental data follow the pseudo-second order better compared to the pseudo-first one.

In view of these given results, we can say that pomegranate peels constitute versatile tools for the treatment of lead poisoning in humans through their polyphenols content and their iron chelating antioxidant activity that inhibit reactive oxygen species generated

during the oxidative stress induced by lead. In addition and in terms of adsorption, pomegranate peels as an agro-waste, can be used efficiently and advantageously in removing lead pollutant from effluents, which contributes in the protection of the environment from its toxic effects. Finally, the effective adsorption-desorption of lead at interface of these biomasses as sorbents is another advantage in terms of their reuse and effluents treatment costs.

Acknowledgments

We would like to deeply thank the ENPEC (National Company of Electrochemical Products) of Setif (Algeria) for their availability and fruitful cooperation. Particular gratitude is addressed to the managers of the analysis laboratory for their friendliness and helpfulness during the performance of the work by atomic absorption.

Conflict of Interest

The authors declare that there are no conflicts of interest.

References

1. BRIFFA J., SINAGRA E., BLUNDEL R. Heavy metal pollution in the environment and their toxicological effects on humans. Heliyon. **6** (9), e04691, **2020**.
2. PRATIKSHA K., TOMAR S., SHARMA P. Effects of Environmental Pollution on Human Health. Agriculture and Food: e-Newsletter. **2** (8), 982, **2020**.
3. DÖKMECI A.H. Environmental Impacts of Heavy Metals and Their Bioremediation. In Heavy Metals - Their Environmental Impacts and Mitigation; Nazal M., Zhao H., Eds., IntechOpen, London, **2020**.
4. YEDJOU C.G., TCHOUNWOU C.K., HAILE S., EDWARDS F., TCHOUNWOU P.B. N-acetyl-cysteine protects against DNA damage associated with lead toxicity in HepG2 cells. Ethnicity and Disease. **20** (1 Suppl 1), S1-101, **2010**.
5. MARKOWITZ M. Lead Poisoning: An Update. Pediatrics in Review. **42** (6), 302, **2021**.
6. ABDULLA M. Lead, chapter 13. In Essential and Toxic Trace Elements and Vitamins in Human Health, 1st ed.; Prasad A.S., Brewer G.J., Eds., Academic Press, Netherlands, 181, **2020**.
7. AL OSMAN M., YANG F., MASSEY I.Y. Exposure routes and health effects of heavy metals on children. BioMetals. **32**, 563, **2019**.
8. LUZ A.L., WU X., TOKAR E.J. Chapter One - Toxicology of Inorganic Carcinogens. Advances in Molecular Toxicology. **12**, 1, **2018**.
9. BEYERSMANN D., HARTWIG A. Carcinogenic metal compounds: recent insight into molecular and cellular mechanisms. Archives of Toxicology. **82** (8), 493, **2008**.
10. WONG M.H. Environmental Contamination: Health Risks and Ecological Restoration. Ecotoxicology. **22** (7), 1183, **2013**.
11. TUREL I., KLJUN J. Interactions of Metal Ions with DNA, Its Constituents and Derivatives. Current Topics in Medicinal Chemistry. **11** (21), 2661, **2011**.
12. QASEM N.A.A., MOHAMMED R.H., LAWAL D.U. Removal of heavy metal ions from wastewater: a comprehensive and critical review. npj Clean Water. **4** (36), **2021**.
13. GHAHREMANI A., MANTEGHIAN M., KAZEMZADEH H. Removing lead from aqueous solution by activated carbon nanoparticle impregnated on lightweight expanded clay aggregate. Journal of Environmental Chemical Engineering. **9** (1), 104478, **2021**.
14. OMER A.M., DEY R., ELTAWEIL A.S., ABD EL-MONAEM E.M., ZIORA Z.M. Insights into recent advances of chitosan-based adsorbents for sustainable removal of heavy metals and anions. Arabian Journal of Chemistry. **15** (2), 103543, **2022**.
15. HAGHIGHI H.K., IRANNAJAD M., MOHAMMADJAFARI A. Thermodynamic and kinetic studies of heavy metal adsorption by modified nano-zeolite. Geosystem Engineering. **24** (2), 101, **2021**.
16. ÜNER O., KÖRÜKÇÜ B.C., ÖZCAN C. Adsorption application of activated carbon from ripe black locust seed pods for wastewater taken from Ergene River, Turkey. International Journal of Environmental Analytical Chemistry. 1, **2021**.
17. WOŁOWIEC M., KOMOROWSKA-KAUFMAN M., PRUSS A., RZEPA G., BAJDA T. Removal of Heavy Metals and Metalloids from Water Using Drinking Water Treatment Residuals as Adsorbents: A Review. *Minerals*. **9** (8), 487, **2019**.
18. VILARDI G., OCHANDO-PULIDO J.M., VERDONE N., STOLLER M., DI PALMA L. On the removal of hexavalent chromium by olive stones coated by iron-based nanoparticles: Equilibrium study and chromium recovery. Journal of Cleaner Production. **190**, 200, **2018**.
19. ŠOŠTARIĆ T.D., PETROVIĆ M.S., PASTOR F.T., LONČAREVIĆ D.R., PETROVIĆ J.T., MILOJKOVIĆ J.V., STOJANOVIĆ M.D. Study of heavy metals biosorption on native and alkali-treated apricot shells and its application in wastewater treatment. Journal of Molecular Liquids. **259**, 340, **2018**.
20. ASHFAQ A., NADEEM R., BIBI S., RASHID U., HANIF A., JAHAN N., ASHFAQ Z., AHMED Z., ADIL M., NAZ M. Efficient Adsorption of Lead Ions from Synthetic Wastewater Using Agrowaste-Based Mixed, Biomass (Potato Peels and Banana Peels). Water. **13** (23), 3344, **2021**.
21. AFOLABI F.O., MUSONGE P., BAKARE B.F. Evaluation of Lead (II) Removal from Wastewater Using Banana Peels: Optimization Study. Polish Journal of Environmental Studies. **30** (2), 1487, **2021**.
22. ADDALA A., BELATTAR N., ELEKTOROWICZ M. *Nigella sativa* L. Seeds Biomass as a Potential Sorbent in Sorption of Lead from Aqueous Solutions and Wastewaters. Oriental Journal of Chemistry. **34** (2), 638, **2018**.
23. LE K., CHIU F., NG K. Identification and quantification of antioxidants in *Fructus lycii*. Food Chemistry. **105** (1), 353, **2007**.
24. GULZAR I.I., AVEEN F.J., BANAR M.I. Evaluation of antioxidant activity, phenolic, flavonoid and ascorbic acid contents of three edible plants from Erbil/Kurdistan. Tikrit Journal of Pure Science. **18** (3), 46, **2013**.
25. BEN-ALI S., JAOUALI I., SOUISSI-NAJAR S., OUEDERNI A. Characterization and adsorption capacity

of raw pomegranate peel biosorbent for copper removal. Journal of Cleaner Production. **142** (4), 3809, **2017**.
26. TARBAOUI M., OUMAM M., FOURMENTIN S., BENZINA M., BENNAMARA A., ABOURRICHE A. Development of A New Biosorbent Based on The Extract Residue of Marine Alga *Sargassum Vulgare*: Application in Biosorption of Volatile Organic Compounds. *World Journal of Innovative Research*. **1** (1), 1, **2016**.
27. BOUNAAS M., BOUGUETTOUCHA A., CHEBLI D., REFFAS A., HARIZI i., ROUABAH F., AMRANE A. High efficiency of methylene blue removal using a novel low-cost acid treated forest wastes, *Cupressus semperirens* cones: Experimental results and modeling. Particulate Science and Technology. **37** (4), 504, **2019**.
28. BOEHM H.P. Some Aspects of the Surface Chemistry of Carbon Blacks and Other Carbons. Carbon. **32** (5), 759, **1994**.
29. ELHLELI H., MANNAI F., BEN MOSBAH M., KHIARI R., MOUSSAOUI Y. Biocarbon Derived from *Opuntia ficus indica* for *p*-Nitrophenol Retention. *Processes*. **8** (10), 1242, **2020**.
30. OBAID S.A. Journal of Physics: Conference Series. **1664**, 012011, **2020**.
31. LANGMUIR I. The Adsorption of Gases on Plane Surfaces of Glass, Mica and Platinum. Journal of the American Chemical Society. **40** (9), 1361, **1918**.
32. EDET U.A., IFELEBUEGU A.O. Kinetics, Isotherms, and Thermodynamic Modeling of the Adsorption of Phosphates from Model Wastewater Using Recycled Brick Waste. Processes. **8** (6), 665, **2020**.
33. FREUNDLICH H. Über die Struktur der Kolloidteilchen und über den Aufbau von Solen und Gelen. Berichte der Deutschen Chemischen Gesellschaft. **61 (10)**, 2219, **1928**.
34. WANG J., GUO X. Adsorption kinetic models: Physical meanings, applications, and solving methods. Journal of Hazardous Materials. **390**, 122156, **2020**.
35. LAGERGREN S. Zur Theorie der Sogenannten Adsorption Gelöster Stoffe, Kungliga Svenska Vetenskapsakademiens. Handlingar. **24** (4), 1, **1898**.
36. ABEDI M., SALMANI M.H., MOZAFFARI S.A. Adsorption of Cd ions from aqueous solutions by iron modified pomegranate peel carbons: kinetic and thermodynamic studies. International Journal of Environmental Science and Technology. **13**, 2045, **2016**.
37. HO Y.S., MCKAY G. Pseudo-second order model for sorption processes. Process Biochemistry. **34** (5), 451, **1999**.
38. KENNAS A., AMELLAL-CHIBANE H. Comparison of five solvents in the extraction of phenolic anti-oxidants from pomegranate (*Punica granatum* L.) peel. The North African Journal of Food and Nutrition Research. **3** (5), 140, **2019**.
39. FOURATI M., SMAOUI S., BEN HLIMA H., ELHADEF K., CHAKCHOUK MTIBAA A., MELLOULI L. Variability in phytochemical contents and biological potential of pomegranate (*Punica granatum*) peel extracts: toward a new opportunity for minced beef meat preservation. Journal of Food Quality. **2020**, 1, **2020**.
40. ORAK H.H., YAGAR H., ISBILIR S.S. Comparison of antioxidant activities of juice, peel, and seed of pomegranate (*Punica granatum* L.) and inter-relationships with total phenolic, Tannin, anthocyanin, and flavonoid contents. Food Science and Biotechnology. **21** (2), 373, **2012**.
41. FAWOLE O.A., MAKUNGA N.P., OPARA U.L. Antibacterial, antioxidant and tyrosinase-inhibition activities of pomegranate fruit peel methanolic extract. BMC Complementary and Alternative Medicine. **12** (1), 200, **2012**.
42. RAO R.A.K., REHMAN F. Adsorption of Heavy Metal Ions on Pomegranate (*Punica Granatum*) Peel: Removal and Recovery of Cr(VI) Ions from a Multi-metal Ion System. Adsorption Science and Technology. **28** (3), 195, **2010**.
43. AY C.O., OZCAN A.S., ERDOĞAN Y., OZCAN A. Characterization of Punica *granatum* L. peels and quantitatively determination of its biosorption behavior towards lead(II) ions and Acid Blue 40. Colloids and Surfaces B: Biointerfaces. **100**, 197, **2012**.
44. SILVEIRA M.B., PAVAN F.A., GELOS N.F., LIMA E.C., DIAS S.L.P. *Punica Granatum* Shell Preparation, Characterization, and Use for Crystal Violet Removal from Aqueous Solution. CLEAN - Soil Air Water. **42** (7), 939, **2014**.
45. WANG X., WANG L., WANG Y., TAN R., KE X., ZHOU X., GENG J., HOU H., ZHOU M. Calcium Sulfate Hemihydrate Whiskers Obtained from Flue Gas Desulfurization Gypsum and Used for the Adsorption Removal of Lead. Crystals. **7** (9), 270, **2017**.
46. MOGHADAM M.R., NASIRIZADEH N., DASHTI Z., BABANEZHAD E. Removal of Fe(II) from aqueous solution using pomegranate peel carbon: equilibrium and kinetic studies. International Journal of Industrial Chemistry. **4** (19), **2013**.
47. GÜZEL F., AKSOY Ö., SAYĞILI G. Application of Pomegranate (*Punica granatum*) Pulp as a New Biosorbent for the Removal of a Model Basic Dye (Methylene Blue). World Applied Sciences Journal. **20** (7), 965, **2012**.
48. GRABI H., DERRIDJ F., LEMLIKCHI W., GUÉNIN E. Studies of the potential of a native natural biosorbent for the elimination of an anionic textile dye Cibacron Blue in aqueous solution. Scientific Reports. **11** (9705), **2021**.
49. PAVAN F.A., MAZZOCATO A.C, JACQUES R.A., DIAS S.L.P. Ponkan Peel: A Potential Biosorbent for Removal of Pb(II) Ions from Aqueous Solution. Biochemical Engineering Journal. **40** (2), 357, **2008**.
50. ISAAC C.P.J., SIVAKUMAR A. Removal of lead and cadmium ions from water using *Annona squamosa* shell: kinetic and equilibrium studies. Desalination and Water Treatment. **51** (40-42), 7700, **2013**.
51. ANWAR J., SHAFIQUE U., ZAMAN W., SALMAN M., DAR A., ANWAR S. Removal of Pb(II) and Cd(II) from water by adsorption on peels of banana. Bioresource Technology. **101** (6), 1752, **2010**.
52. EL-ASHTOUKHY E.S.Z., AMIN N.K., ABDELWAHAB O. Removal of lead (II) and copper (II) from aqueous solution using pomegranate peel as a new adsorbent. Desalination. **223** (1-3), 162, **2008**.